Journal of Alloys and Compounds 506 (2010) 745–748

Contents lists available at ScienceDirect

Journal of Alloys and Compounds

journal homepage: www.elsevier.com/locate/jallcom

Fabrication, properties and laser performance of Ho:YAG transparent ceramic

W.X. Zhang[a,b], J. Zhou[a,b], W.B. Liu[a], J. Li[a], L. Wang[a,b], B.X. Jiang[a], Y.B. Pan[a,*], X.J. Cheng[c], J.Q. Xu[c]

[a] Key Laboratory of Transparent and Opto-functional Advanced Inorganic Materials, Shanghai Institute of Ceramics, Chinese Academy of Sciences, Shanghai 200050, PR China
[b] Graduate School of the Chinese Academy of Sciences, Beijing 100039, PR China
[c] Shanghai Institute of Optics and Fine Mechanics, Chinese Academy of Sciences, Shanghai 201800, PR China

ARTICLE INFO

Article history:
Received 12 May 2010
Received in revised form 7 July 2010
Accepted 7 July 2010
Available online 15 July 2010

Keywords:
Ho:YAG ceramic
Optical properties
Microstructure
Laser performance

ABSTRACT

Highly transparent Ho:YAG ceramic was successfully fabricated by solid-state reaction and vacuum sintering. The optical properties, the microstructure and the laser performance of the Ho:YAG ceramic were investigated. Ho:YAG ceramic with the average grain size of ~15 μm was obtained by sintering at 1760 °C for 20 h. The in-line transmittances in the visible region and the infrared region were both over 80%. No pores, impurities and secondary phases were detected in the grains and at the grain boundaries. The 1 at.% Ho:YAG ceramic slab (1.5 mm × 10 mm × 18 mm) was end-pumped by a Tm-YLF laser at 1910 nm. The maximum output power of 1.95 W was yielded with a slope efficiency of 44.19% and Tm to Ho optical–optical efficiency was 24% at 2091 nm.

1. Introduction

In recent years, an increasing interest has been focused on the solid-state lasers operating in the eye-safe spectral region near 2 μm because of their varied applications such as optical communications, coherent laser radar, atmospheric sensing and medical equipment [1–4]. Also, high-power quasi-continuous wave (QCW) 2 μm lasers are efficient pump sources of optical parametric oscillators (OPOs) and optical parametric amplifiers (OPAs).

Currently two technologies are in wide use—diode-pumped 1.9 μm thulium (Tm^{3+}) and 2.1 μm holmium (Ho^{3+}) lasers. The performance of the Tm^{3+} in $Y_3Al_5O_{12}$ (YAG)/$YAlO_3$ (YAP)/$Gd_3Ga_5O_{12}$ (GGG) single crystal has been widely studied and the laser operation has been successfully realized [4–7]. Diode-pumped Tm:YAG ceramic laser also has been studied in our previous work [8]. Ho^{3+} lasers are used as pump sources for non-linear optics to generate mid-infrared radiation in the spectral range of 3–5 μm, for lidar applications as their emission wavelengths are less affected by the atmospheric water vapor absorption than those of Tm^{3+} lasers, in medicine and for plastic welding [9]. Moreover, direct resonant pumping Ho $^5I_7$ manifold offers the advantages of high slope efficiency (70% in Ho:$YLiF_4$) [10], minimal heating due to low quantum defect of less than 10% between pump and laser.

The performance of the Ho:YAG single crystal has been widely studied [11,12] and the laser operation has been successfully realized [13–18]. Holmium-doped yttrium aluminum garnet (Ho:YAG) ceramic is the promising material of choice for 2.1 μm applications due to its well-known excellent thermo-mechanical properties and advantages compared with Ho:YAG single crystal (for example: ease of fabrication, less cost, mass production, feasibility of large size, high holmium concentration, etc.). The laser performance of Ho:YAG ceramic has been reported in Dr. Cheng's work with the specimen we provided [19]. And to the best of our knowledge, fabrication and properties of highly transparent Ho:YAG ceramic has not been reported yet.

Ho:YAG does not have any suitable absorption feature in the traditional diode laser wavelength window of 785–980 nm, so that Ho:YAG cannot be directly pumped by traditional diode lasers. Using Tm-doped laser operating at approximate 1.9 μm direct resonant pumping Ho $^5I_7$ manifold offers the advantages of high quantum efficiency, minimal heating due to low quantum defect between pump and laser of ~10%, and reduced up-conversion losses caused by Tm sensitized. Therefore, this approach has the advantage of very low quantum defect heating with the result that high lasing efficiencies are attainable.

Available room-temperature pump sources for Ho are the Tm laser in the hosts YAG, $YLiF_4$ (YLF), and YAP. The absorption spectrum of Tm:YLF falls within the emission spectrum of commercially available laser diodes emitting peak of 792 nm. The emission spectrum of Tm:YLF matches well with the relatively broad absorption spectrum of Ho:YAG. Therefore, Tm:YLF laser allows relatively low

* Corresponding author at: Shanghai Institute of Ceramics, Chinese Academy of Sciences, 1295 Ding-Xi Road, Shanghai 200050, PR China.
Tel.: +86 21 52412820; fax: +86 21 52413903.
E-mail address: ybpan@mail.sic.ac.cn (Y.B. Pan).

0925-8388/$ – see front matter © 2010 Elsevier B.V. All rights reserved.
doi:10.1016/j.jallcom.2010.07.059

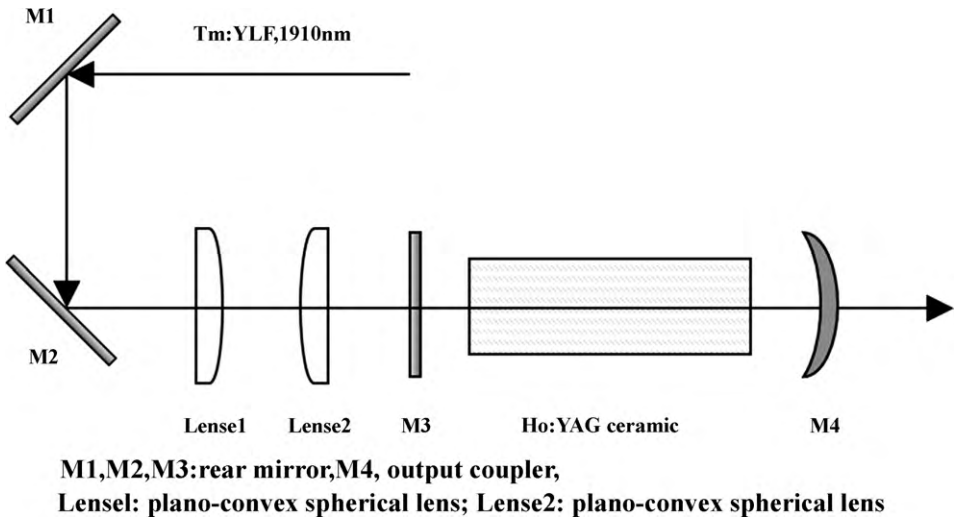

Fig. 1. The scheme of the Ho:YAG ceramic laser experiment.

brightness diode pump sources to be used and efficiently pumping Ho:YAG [20,21].

In this paper, highly transparent Ho:YAG ceramic was successfully fabricated by a simple solid-state reaction method and vacuum-sintering technology. The microstructure, the spectral characteristics and room-temperature laser actions of Tm-YLF laser pumped Ho:YAG ceramic in CW modes were reported in this work.

2. Experimental procedures

2.1. Ceramic fabrication

High-purity powders of α-Al_2O_3 (99.99%, Shanghai Wusong Chemical Co. Ltd., Shanghai, China), Y_2O_3 (99.99%, Shanghai Yuelong New Materials Co. Ltd., Shanghai, China), and Ho_2O_3 (99.99%, Conghua Jianfeng Rare-Earth Co. Ltd., Guangzhou, China) were used as starting materials. These powders were blended according to the stoichiometric ratio of 1 at.% Ho:YAG and ball-milled with high-purity corundum balls for in ethanol 10 h, with a binder and addition of 0.6 wt% tetraethyl orthosilicate (TEOS) as a sintering aid. Then, the alcohol solvent was removed by drying the milled slurry at 80 °C for 4 h in oven. The dried powder mixture was ground and sieved through 200-mesh screen. After removing the organic component by calcining at 500–800 °C for 2 h, the powder mixture was dry-pressed with a low pressure into Φ25 mm disks in a steel mold and then cold-isostatic-pressed at 250 MPa into green bodies. Then the green bodies were vacuum-sintered at 1760 °C for 20 h. After sintering, the specimens were annealed at 1400 °C for 1 h in air to relieve internal stresses and fill oxygen vacancies formed during the vacuum-sintering process. Finally, highly transparent Ho:YAG ceramics were obtained.

The phase composition of the sample was identified by X-ray diffraction (Model D/MAX-2550V, Rigaku, Tokyo, Japan). The sample mirror-polished on both surfaces was used to measure optical transmittance and absorption spectra (Model U-2800 Spectrophotometer, Hitachi, Tokyo, Japan). For measuring the fluorescence spec-

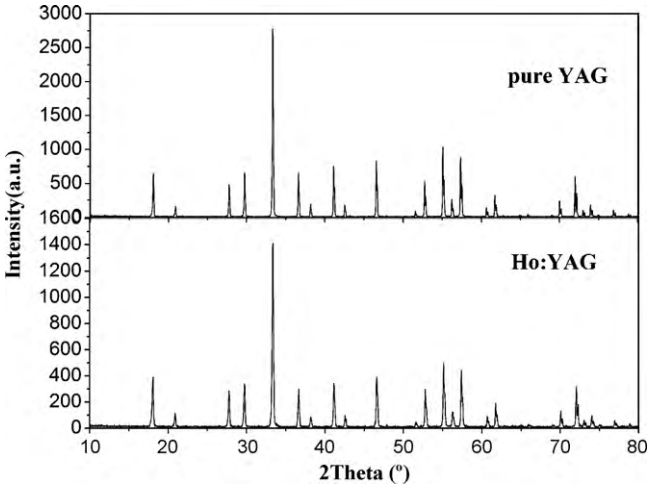

Fig. 2. XRD patterns of pure YAG and Ho:YAG samples.

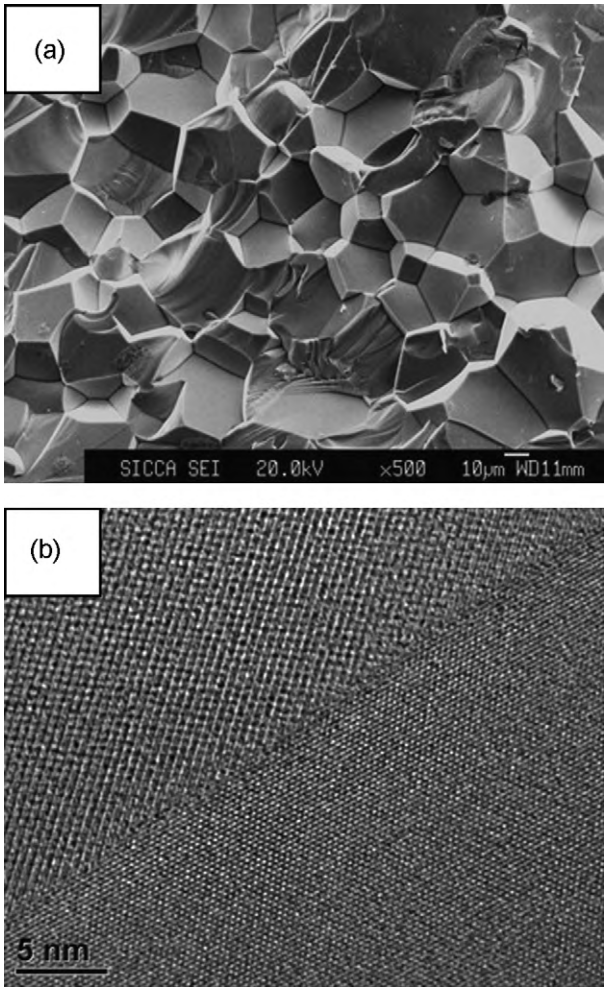

Fig. 3. The EPMA micrograph of the fractured surface (a) and the high-resolution TEM micrograph (HRTEM) of the grain boundary (b) of the Ho:YAG ceramic.

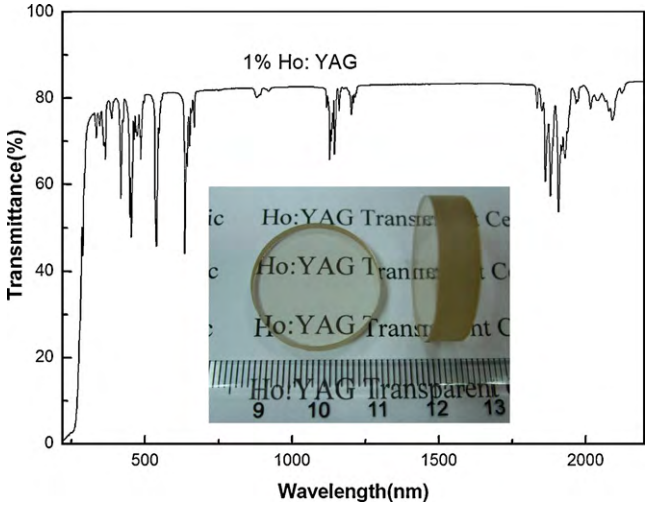

Fig. 4. The transmittance spectrum of mirror-polished 1 at.% Ho:YAG sample. The inset picture is the appearance of the sample.

trum (Model Fluorolog-3, Jobin Yvon, Paris, France), the specimen was excited at 640 nm by the flash lamp. The microstructure of the fractured surface of the sample was observed by electron probe micro-analyzer (EPMA, Model JXA-8100, JEOL, Tokyo, Japan). The microstructure of grain boundary was characterized by a field emission transmission electron microscopy (FETEM, Model EM 2100, JEOL, Tokyo, Japan).

2.2. Laser experiment

Fig. 1 shows a schematic diagram of the experimental setup. The dimension of the sample is 1.5 mm × 10 mm × 18 mm. Both surfaces (1.5 mm × 10 mm) of the Ho:YAG ceramic were mirror-polished, parallel, and coated with an anti-reflection at 1910 nm and 2100 nm. The sample was end-pumped by a Tm-YLF laser with an emission wavelength of around 1910 nm. M1 and M2 were two rear mirrors which were set at 45° angle with the Tm-YLF laser beam and anti-reflection coated at 1910 nm. The laser cavity consisted of two mirrors (M3 and M4), where M3 was anti-reflection coated at 1910 nm and high-reflection coated at 2100 nm, and M4 was the output coupler (OC). The transmittance at 2090 nm and curvature radius of the output coupler is 5%, 400 mm.

3. Results and discussion

Fig. 2 displays the XRD patterns of Ho:YAG and pure YAG ceramic at room temperature. The locations of Ho:YAG peaks are almost the same as that of pure YAG although the strength of peaks is different. That is because that the Ho:YAG ceramic has the same structure as the pure YAG ceramic. The calculated lattice constant for Ho:YAG ceramic is 1.2009 nm, which is quite similar to that of pure YAG ceramic (the calculated lattice constant for pure YAG is 1.2010 nm), because that Ho^{3+} takes the position of Y^{3+} in the lattice structure

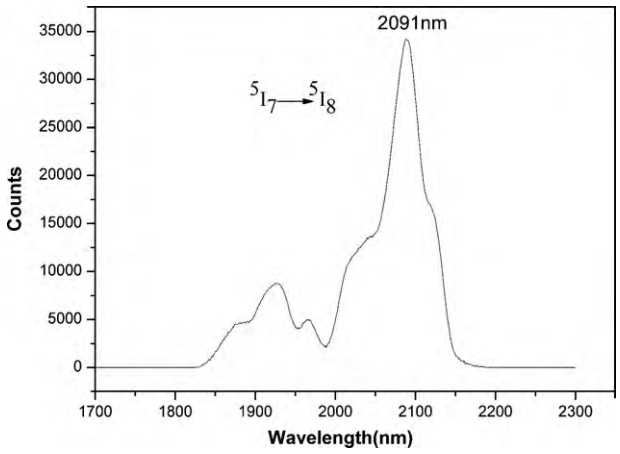

Fig. 6. The fluorescence spectrum of the 1 at.% Ho:YAG ceramic at room temperature.

and the radius of Ho^{3+} (89.4 pm) is just a little smaller than that of Y^{3+} (90 pm).

The EPMA micrograph of fractured surface (Fig. 3(a)) and the high-resolution TEM micrograph (HRTEM) of the grain boundary (Fig. 3(b)) show the microstructure of the Ho:YAG ceramic. As shown, the grain sizes are quite uniform and the average grain size is about 15 μm. The grain boundary is clear and clean. There are no pores, impurities and secondary phases in the grains and at the grain boundary.

From the in-line transmittance spectrum in Fig. 4, we can see that Ho:YAG laser wavelength (around 2.1 μm) is right in the absorption band (1800–2100 nm), which indicates that Ho:YAG laser has a self-absorption process. In this case, normally the Ho^{3+} doping levels should not be above 3% in the Ho:YAG laser material. The inset picture is the appearance of the samples. The samples are highly transparent and the thickness is 5 mm.

The emission spectrum of Tm:YLF (Fig. 5(a)) [22] coincides well with the absorption spectrum of Ho:YAG transparent ceramic (Fig. 5(b)). Both of the peak emission cross-section lines (1.880 and 1.907 μm) in Tm:YLF are well suited to pump Ho:YAG ceramic efficiently. For this work, we use the 1.9 μm Tm:YLF line as a pump source.

Fig. 6 is the room-temperature fluorescence spectrum excited by the flash lamp. The emission region with a peak at 2091 nm is from 1800 nm to 2200 nm which comes from the transition $^5I_7 \rightarrow {}^5I_8$ of the 1% Ho:YAG ceramic. With the fluorescence spectrum, the sample was suitably coated and the laser experiment was well designed in Fig. 1.

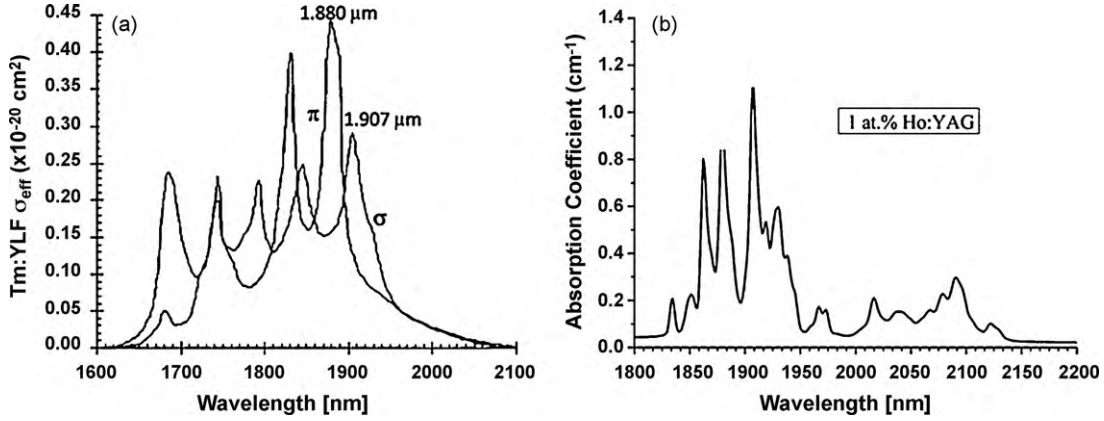

Fig. 5. The effective emission cross-section of Tm:YLF (a) [13] and the absorption spectrum of the Ho:YAG ceramic from 1800 nm to 2200 nm (b).

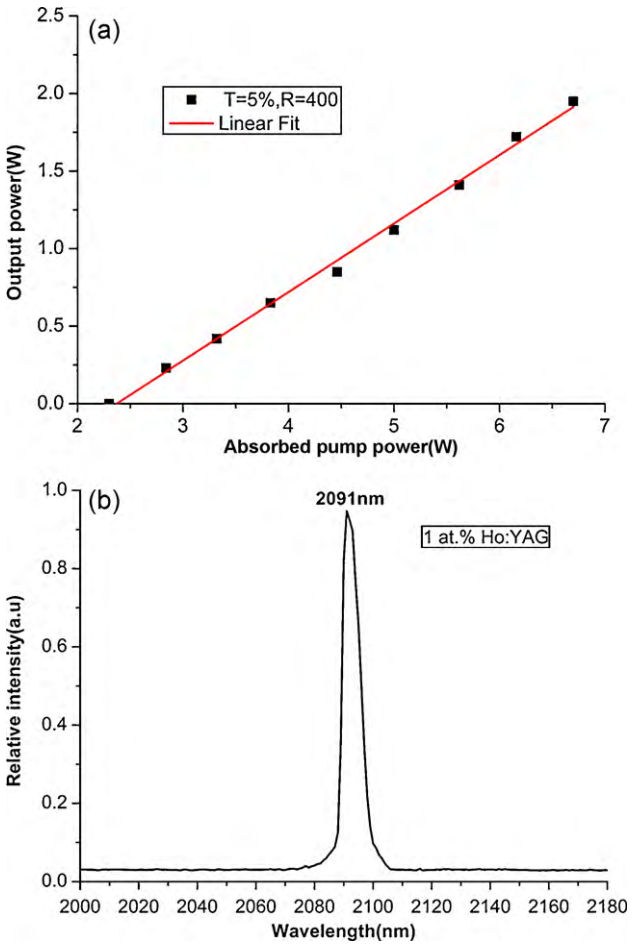

Fig. 7. The laser output power versus the absorbed pump power (a) and the laser spectrum (b) for the 1 at.% Ho:YAG ceramic.

To the best of our knowledge, highly transparent Ho:YAG ceramic is fabricated for the first time in this paper. The Ho:YAG ceramic slab was end-pumped by a Tm-YLF laser. The laser spectrum of the 1 at.% Ho:YAG ceramic is centered at 2091 nm, as shown in Fig. 7(b). Fig. 7(a) illustrates the laser output power versus the absorbed pump power for the 1 at.% Ho:YAG ceramic. The maximum laser output power of 1.95 W has been obtained with only 6.7 W of absorbed Tm pump power. A linear fit to the data yielded a slope efficiency of 44.19% with a threshold of approximately 2.3 W. The Tm:YLF to Ho:YAG optical-to-optical efficiency was 24%. The slope efficiency and optic–optic transformation efficiency of Ho:YAG ceramic yielded in this study are still lower than those of Ho:YAG crystal (the slope efficiency and optic–optic transformation efficiency of Ho:YAG crystal are 57% and 38%, respectively [23]), however, with improvement of ceramic fabrication process and optical quality, Ho:YAG ceramic is a very promising substitute for Ho:YAG crystal in the foreseeable future.

4. Conclusions

Highly transparent Ho:YAG ceramic with average grain size of ~15 μm was obtained by solid-state reaction and vacuum sintering. The grain boundary was clean and no secondary phase was observed. The 1 at.% Ho:YAG ceramic slab was end-pumped by a Tm-YLF laser at 1910 nm. The maximum output power of 1.95 W was obtained with a slope efficiency of 44.19% and Tm to Ho optical-to-optical efficiency of 24% at 2091 nm. The results of the laser experiment show that the quality of such kind of ceramics is good enough to be used as a highly efficient laser material.

Acknowledgments

The authors acknowledge Dr. Xiao-Jin Cheng and Prof. Jian-Qiu Xu for the laser experiment. This work was supported by the 863 project (No. AA03Z523), NSFC (No. 50990300) and the Major Basic Research Programs of Shanghai (No. 07DJ14001).

References

[1] K. Scholle, E. Heumann, G. Huber, Laser Phys. Lett. 1 (2004) 285.
[2] N.D. Vieira Jr., I.M. Ranieri, L.V.G. Tarelho, N.U. Wetter, S.L. Baldochi, L. Gomes, P.S.F. de Matos, W. de Rossi, G.E.C. Nogueira, L.C. Courrol, E.A. Barbosa, E.P. Maldonado, S.P. Morato, J. Alloys Compd. 344 (2002) 231.
[3] M.J. Bader, J. Hocaoglu, S. Walther, M. Seitz, R. Sroka, C.G. Stief, O. Reich, Med. Laser Appl. 24 (2009) 132.
[4] C.T. Wu, Y.L. Ju, Z.G. Wang, Q. Wang, C.W. Song, Y.Z. Wang, Laser Phys. Lett. 5 (2008) 793.
[5] Y.L. Lu, J. Wang, Y. Yang, Y.B. Dai, A.P. Dong, B.D. Sun, J. Alloys Compd. 429 (2007) 296.
[6] Y. Yang, Y.L. Lu, J. Wang, Y.B. Dai, B.D. Sun, J. Alloys Compd. 455 (2008) 1.
[7] H. Zhou, X.H. Ma, G.T. Chen, W.C. Lv, Y. Wang, Z.Y. You, J.F. Li, Z.J. Zhu, C.Y. Tu, J. Alloys Compd. 475 (2009) 555.
[8] W.X. Zhang, Y.B. Pan, J. Zhou, W.B. Liu, J. Li, B.X. Jiang, X.J. Cheng, J.Q. Xu, J. Am. Ceram. Soc. 92 (2009) 2434.
[9] M. Eichhorn, Appl. Phys. B 93 (2008) 269.
[10] F. Wang, D.Y. Shen, D.Y. Fan, Q.S. Lu, Chin. J. Laser 36 (2009) 1727.
[11] A. Wnuk, M. Kaczkan, Z. Frukacz, I. Pracka, G. Chadeyron, M.-F. Joubert, M. Malinowski, J. Alloys Compd. 341 (2002) 353.
[12] S. Edvardsson, D. Åberg, J. Alloys Compd. 303–304 (2000) 280.
[13] N.G. Zakharov, O.L. Antipov, V.V. Sharkov, A.P. Savikin, Quantum Electron. 40 (2010) 98.
[14] S.D. Jackson, A. Sabella, D.G. Lancaster, Quantum Electron. 13 (2007) 567.
[15] A. Hemming, J. Richards, S. Bennetts, A. Davidson, N. Carmody, P. Davies, L. Corena, D. Lancaster, Opt. Commun. (2010), doi:10.1016/j.optcom.2010.05.078.
[16] M. Schellhorn, Appl. Phys. B 85 (2006) 549.
[17] S. So, J.I. Mackenzie, D.P. Shepherd, W.A. Clarkson, J.G. Betterton, E.K. Gorton, J.A.C. Terry, Opt. Express. 14 (2006) 10481.
[18] C. Kieleck, A. Hirth, M. Schellhorn, Proc. SPIE 5989 (2005) 598905.
[19] X.J. Cheng, J.Q. Xu, M.J. Wang, B.X. Jiang, W.X. Zhang, Y.B. Pan, Laser Phys. Lett. 7 (2010) 351.
[20] M. Schellhorn, S. Ngcobo, C. Bollig, Appl. Phys. B 94 (2009) 195.
[21] X.M. Duan, B.Q. Yao, C.W. Song, J. Gao, Y.Z. Wang, Laser Phys. Lett. 5 (2008) 800.
[22] P.A. Budni, M.L. Lemons, J.R. Mosto, E.P. Chicklis, Quantum Electron. 6 (2000) 629.
[23] K. Scholle, P. Fuhrberg, Conf. Lasers and Electro-Optics, San Jose, 2008, paper CTuAA1.